Supplementary Materials for *ST-GEARS: Advancing 3D Downstream Research through Accurate Spatial Information Recovery*

Tianyi Xia[1,2], Luni Hu[1,2], Lulu Zuo[3], Lei Cao[1,2], Yunjia Zhang[1,2], Mengyang Xu[2,4], Qin Lu[2], Lei Zhang[1,2], Taotao Pan[1,2], Bohan Zhang[1,2], Bowen Ma[1,2], Chuan Chen[1,2], Junfu Guo[3], Chang Shi[3], Mei Li[2], Chao Liu[1,2,*], Yuxiang Li[2,5,6,*], Yong Zhang[2,5,6,*], Shuangsang Fang[1,2,*]

1 BGI Research, Beijing 102601, China.
2 BGI Research, Shenzhen 518083, China.
3 BGI, Shenzhen 518083, China.
4 BGI Research, Qingdao 266555, China.
5 BGI Research, Wuhan 430074, China.
6 Guangdong Bigdata Engineering Technology Research Center for Life Sciences, BGI research, Shenzhen 518083, China.

*Correspondence: liuchao3@genomics.cn (C.L.), liyuxiang@genomics.cn (Y.L.), zhangyong2@genomics.cn (Y.Z), fangshuangsang@genomics.cn (S.F)

Supplementary Information

Input by ST-GEARS

Gene expression, cross sectional clustering or annotation, and spatial measuring of different spots across sections are required as input of ST-GEARS.

Granularity Adjusting

Across different ST technologies, some with high resolutions can lead to over millions of input spots, causing computational burden in both time and memory. To deal with the situation, we include spots granularity adjusting as an optional preprocessing step, and we recommend users to turn on this option: when over 3000 spots are included in each section. In granularity adjusting, section area is firstly gridded, with spots squared by each pixel summarized into one single spot, leading to a ST data with coarser resolution than original data. When summarizing within each grid, Unique molecular identifier (UMI) counts of spots is summed to, and the most frequent annotation type or cluster is labelled to the generated one spot. Then ST-GEARS is applied onto the coarser version of data, outputting a registered dataset with coarse resolution. Finally, to recover the original resolution in registration result, the original resolution data is interpolated into the pre-registered and registered coarse dataset, leading to registration result in original resolution (Supplementary Fig. 25).

The strategy enables higher computational efficiency in both anchors computation and geospatial

correction, without compromising accuracy of the reconstructed result. For example, we applied granularity adjusting on Mouse hippocampus dataset and ran ST-GEARS on original dataset as well as binned dataset by bin size of respectively 30 and 40 μm. Both time and memory by ST-GEARS were much lower on binned dataset than on original resolution (Supplementary Fig. 26). Lower computational cost was achieved by higher bin size. By comparing registration result through granularity adjusting and direct registration, the coefficient of determination (R^2) remains over 0.98 across all coordinates and sections, on both bin sizes (Supplementary Fig. 27, Supplementary Fig. 28), indicating that accuracy is not compromised by granularity adjusting option.

Across all studied applications, we applied granularity adjusting onto Mouse brain dataset, summarizing each cell's mRNA expression into its belonging 200 μm wide pixels(Supplementary Fig. 23a).

Data Preprocessing

For each summarized or raw spot, both gene expression and geospatial profile are utilized by ST-GEARS as its input. UMI counts responsible for gene expression profile are linearly scaled to 0 to 10000, before log normalization.

Parameter Settings

To provide optimum flexibility for users, we expose multiple parameters of ST-GEARS method as being tunable, such as the start and end index of section list to conduct registration. However, most of them are exposed for users to conveniently conduct the process up to their own will, not to tune the process for a successful result.

There are only 3 parameters whose values were specifically assigned in our application cases, including 'uniform weight', 'label_col', and 'pixel_size' (Supplementary Table 1). 'uniform_weight' specifies whether the Distributive Constraints will be adopted in the registration. Value of False indicates the adoption of the setting, while vice versa. The guidance of when to adopt Distributive Constraints is listed in the section below. As input required by ST-GEARS is stored within data type of anndata.AnnData, 'label_col' is required to be set to the name of column in .obs of the AnnData, where clustering information or annotation type is stored. 'pixel_size' indicates step length on width and height when generating elastic field based on spatial coordinates data. The suggested value is the average distance between closest spots or cells.

Reconstruct samples with different constraints settings

We introduced Distributive Constraints in ST-GEARS to assign different levels of emphasis on different groups of spots, for an enhanced anchor and therefore reconstruction accuracy. However, in general, Distributive Constraints may not be helpful upon extreme scenarios with vast grouping information changes across sections, or absence of reliable grouping information. For example, we applied Distributive Constraints on registration and reconstruction of DLPFC, Drosophila embryo, Drosophila larva and Mouse hippocampus. However, on Mouse brain dataset, we did not adopt the setting, because a vast changing of cell types constitution was witnessed across sections with large distance of 200 μm. In such a circumstance, a distributive emphasis on spots according to cell types were not expected to function equally well with other applications, since it impedes anchors

generation on spots with relative similar expressions but assigned to different annotation types.

In the practical perspective, to decide if Distributive Constraints shall be applied or not, we suggest users to calculate probabilistic distribution of number of spots on different clusters or annotations for each section (Supplementary Fig. 29), then measure Kullback-Leibler (KL) divergence of the distribution between closest section pairs (Supplementary Fig. 30). If the maximum KL divergence remains below 1, Distributive Constraints is suggested to be adopted. However, if the maximum KL divergence exceeds 1, users are encouraged to try ST-GEARS without Distributive Constraints. For example, in our application cases, the maximum KL divergence remains below 1 for both Mouse hippocampus and Drosophila embryo (Supplementary Table 2), and Distributive Constraints was adopted in registration. While in Mouse brain dataset, the value reached 1.448 and the option was excluded during registration. The maximum KL divergence calculation method is also provided by ST-GEARS' GitHub respository.

Benchmarking

To implement benchmarking analysis on PASTE, PASTE2 and GPSA, datasets were preprocessed as according to the requirements of the respective methods. Spots granularity adjusting was applied onto the Mouse brain dataset as input of the three methods, to maintain the same data size and granularity with ST-GEARS. Parameters were set to default values during the computation of the methods.

Supplementary Figures

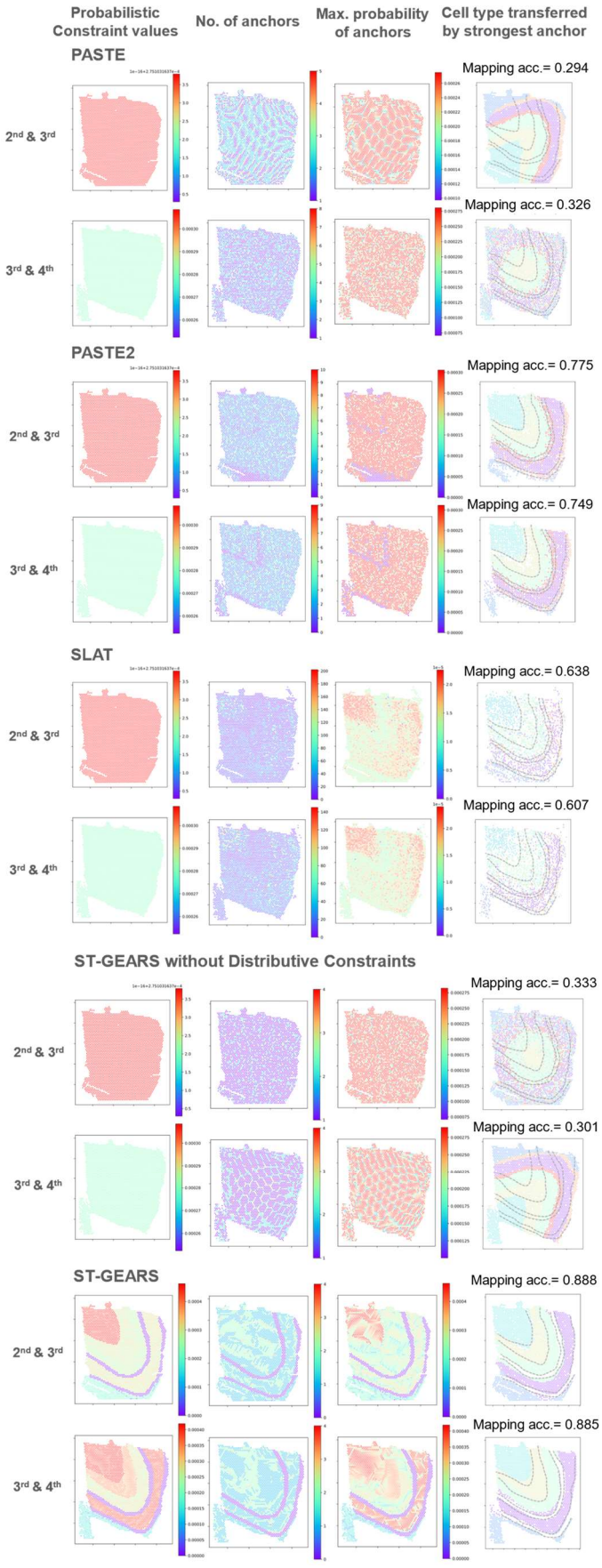

Supplementary Fig. 1: **Distributive emphasis of different cell types of the 2nd to 4th section of DLPFC causes the advanced anchor accuracy.** From the 1st to the 4th column are presented probabilistic constraints settings in problem formulating, no. of anchors computed on each spot, max. anchor probability value computed of each spot, and annotated cell types on the next sections mapped back to its previous sections through computed anchors, with mapping accuracy marked. The distinction of different cell types on the sections are marked by dotted lines. 1st and 2nd row show analysis results of PASTE, 3rd and 4th show results of PASTE2, 5th and 6th row show results of SLAT, 7th and 8th row show results of ST-GEARS without distributive constraints settings, and 9th and 10th rows show results of ST-GEARS with distributive constraints settings. In the results of each method, the upper row presents result of the 2nd and the 3rd sections, while the lower row presents results of the 3rd and 4th sections. As ST-GEARS adopts distributive constraints, it generates relatively more and higher probabilistic anchors on cell types with higher expression consistency across sections, and hence it produces anchors with higher mapping accuracy. Source data are provided as a Source Data file.

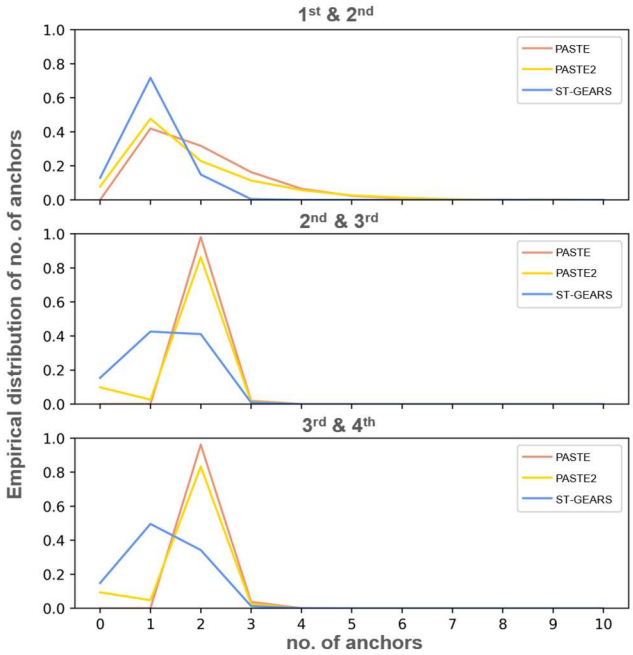

Supplementary Fig. 2: **Suppression of anchors generation on certain spots by ST-GEARS.** Shown here is the comparison of number of anchors distribution of DLPFC dataset computed by PASTE, PASTE2 and ST-GEARS. Each y value shows fraction of no. of anchors specified on x. Different from PASTE, certain percentage of spots have zero anchors generated by ST-GEARS. Source data are provided as a Source Data file.

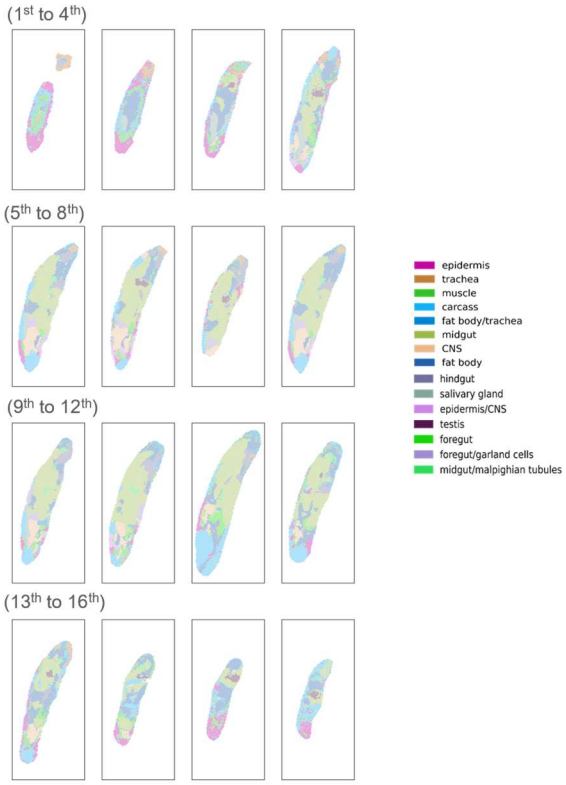

Supplementary Fig. 3: **Individual sections of Drosophila larva generated by rigid registration of ST-GEARS.** Source data are provided as a Source Data file.

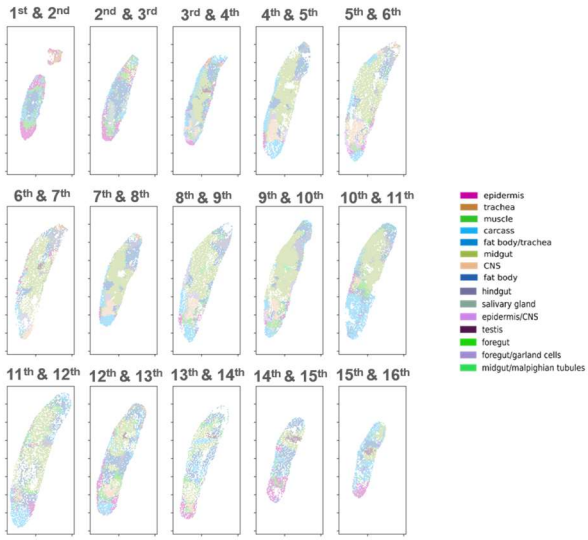

Supplementary Fig. 4: **Anchors correctly connect spots of Drosophila larva with same annotations.** The figure shows annotated cell types of next sections of Drosophila larva mapped back to their previous sections through computed anchors generated by ST-GEARS. The result corresponds well to original cell type distributions of the previous sections, indicating anchors connect spots with same annotations. Source data are provided as a Source Data file.

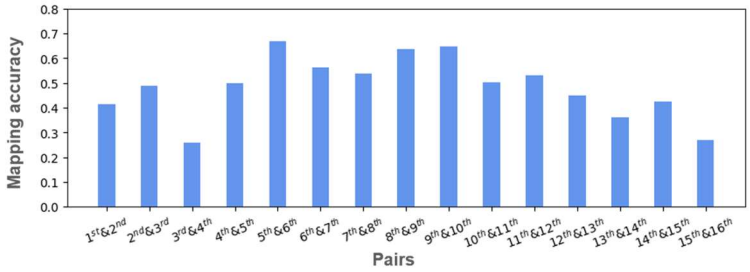

Supplementary Fig. 5: **Mapping accuracy of ST-GEARS on Drosophila larva.** Source data are provided as a Source Data file.

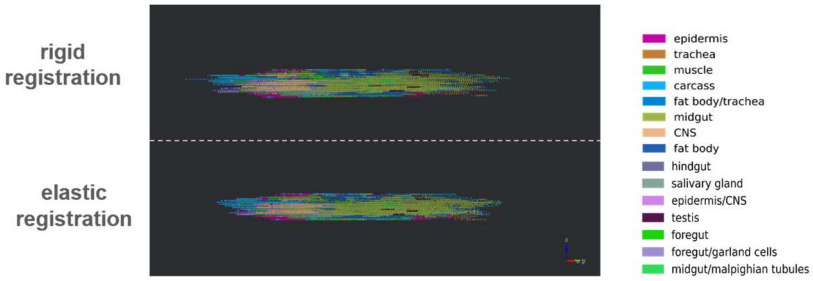

Supplementary Fig. 6: **Cell types of cross sections along Anterior-Posterior(A-P) of Drosophila larva.** Top row presents aligned results by rigid registration, and bottom row presents recovered coordinates by elastic registration, which is appended to rigid registration process. Source data are provided as a Source Data file.

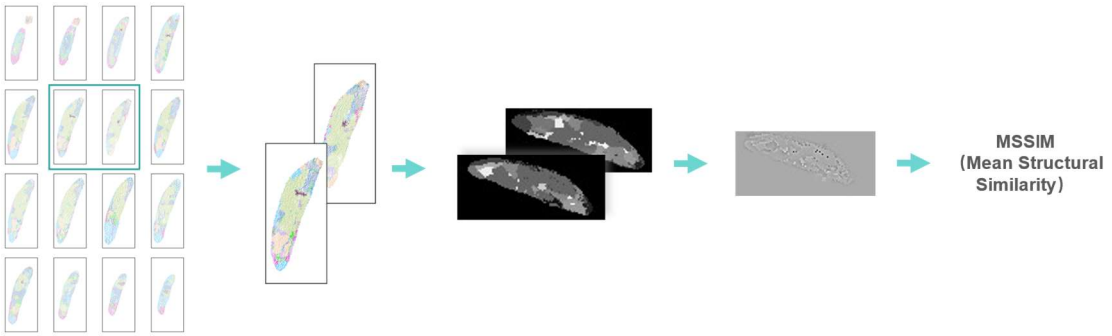

Supplementary Fig. 7: **Calculation of MSSIM index.** To score the registration result of multiple sections, structurally consistent pairs are picked up, and pixeled, with cell type that occur most times in each pixel representing the cell type of the pixel. Cell types are then transformed to grayscales, with different cell types taking different gray scales. Image MSSIM score of pairs is then calculated, representing MSSIM score of the registered pairs. Source data are provided as a Source Data file.

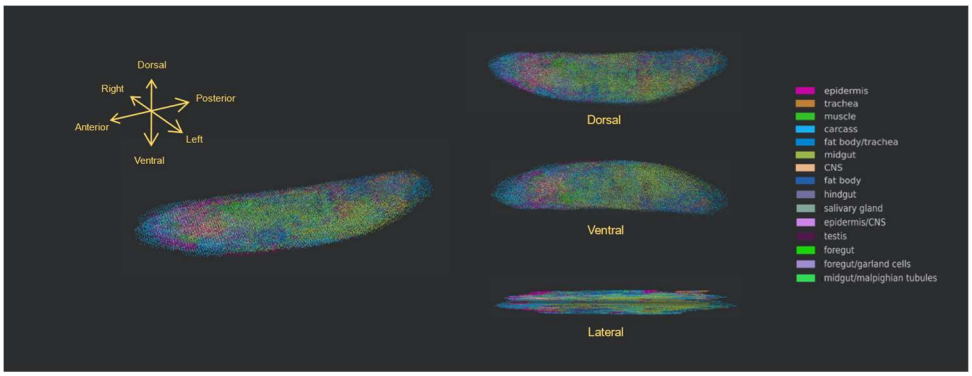

Supplementary Fig. 8: **Elastic process registers Drosophila sections by recovering its *in situ* geo-spatial profile.** Shown here are stacked sections of Drosophila larva generated by elastic registration appended to rigid registration of ST-GEARS, in perspective, dorsal, ventral, and lateral views. Source data are provided as a Source Data file.

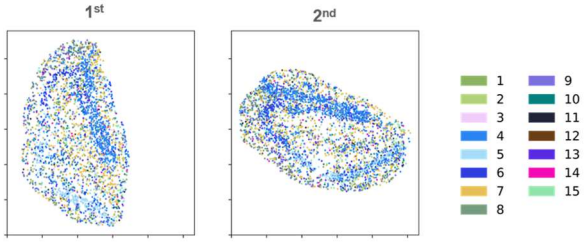

Supplementary Fig. 9: **Sagittal Mouse hippocampus sections before registration.** Source data are provided as a Source Data file.

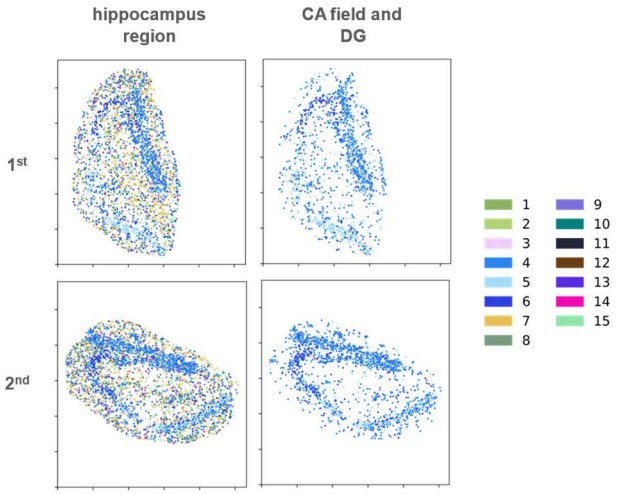

Supplementary Fig. 10: **Cornu Ammonis (CA) fields and Dentate Gyrus (DG) extraction of sagittal Mouse hippocampus sections.** Top row presents the 1st section of Mouse hippocampus, and bottom row represents the 2nd section. Left column presents all spots on the sections, while right column presents filtered spots that belong to CA fields and DG. Source data are provided as a Source Data file.

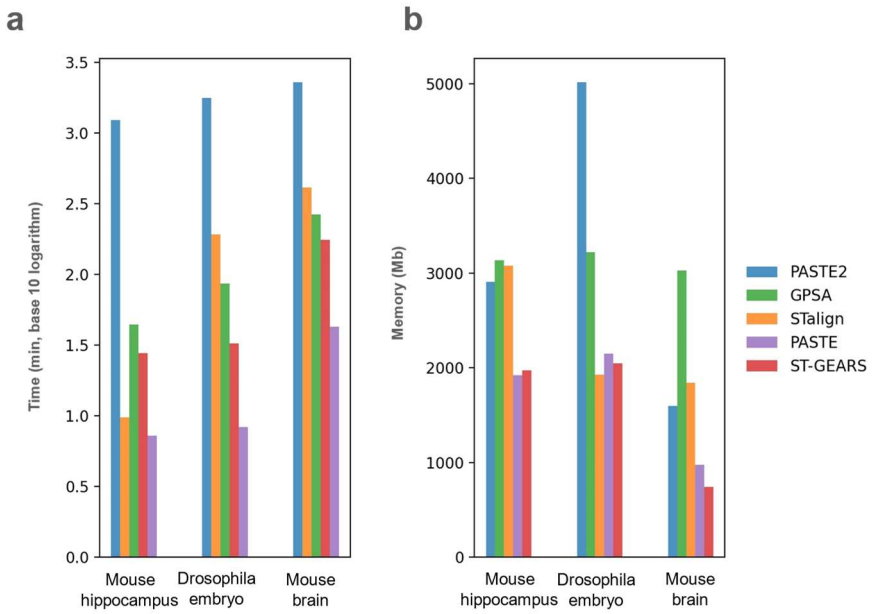

Supplementary Fig. 11: **Time and peak memory consumption of PASTE, PASTE2, GPSA, STalign and ST-GEARS, respectively on Mouse hippocampus, Drosophila embryo and Mouse brain datasets.** Shown in (a) is the time consumption comparison and shown in (b) is the peak memory. Source data are provided as a Source Data file.

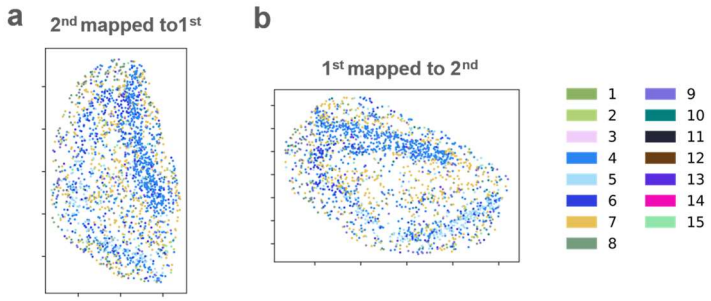

Supplementary Fig. 12: **Anchors correctly connect spots of Mouse hippocampus with same annotations. (a)** Annotated cell types of the 2nd section mapped back the 1st section through computed anchors generated by ST-GEARS. (b) Similar to (a), but cell types of the 1st section mapped to the 2nd. The result corresponds well to original cell type distributions of the sections, which means anchors connect spots with same annotations. Source data are provided as a Source Data file. Source data are provided as a Source Data file.

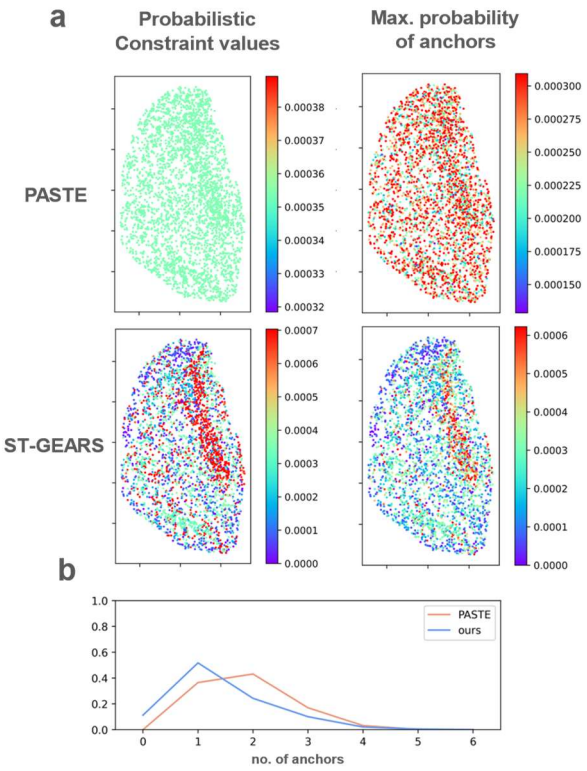

Supplementary Fig. 13: **Distributive emphasis of different cell types of Mouse hippocampus induces distributive anchors by ST-GEARS.** (a) In contrast to PASTE, ST-GEARS assigns distributive probabilistic constraints on different cell types of Mouse hippocampus as shown on the 1st row. By result, its generated maximum probabilities of spots' anchors are different across cell types, compared to PASTE, as shown on the 2nd row. (b) Different from PASTE, certain percentage of spots have zero anchors generated by ST-GEARS. Source data are provided as a Source Data file.

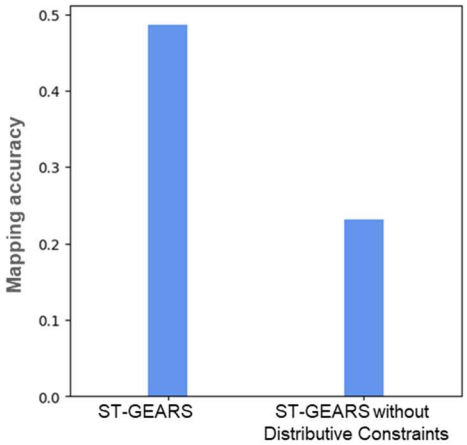

Supplementary Fig. 14: **Distributive Constraints in ST-GEARS enhances mapping accuracy of Mouse hippocampus.** Shown here is the comparison of mapping accuracy of ST-GEARS result, and result of ST-GEARS with Distributive Constraints (DC) excluded, when registering Mouse hippocampus data. The accuracy index is higher upon DC adopted. Source data are provided as a Source Data file.

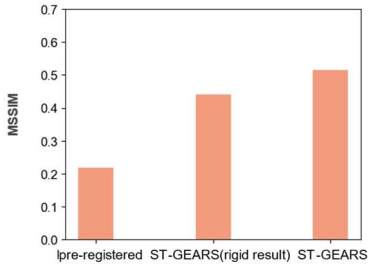

Supplementary Fig. 15: **Elastic registration further improves registration result of Mouse hippocampus based on rigid registration.** Shown here is the MSSIM index of pre-registered, rigid registered and elastic registered section pair of Mouse hippocampus. Source data are provided as a Source Data file.

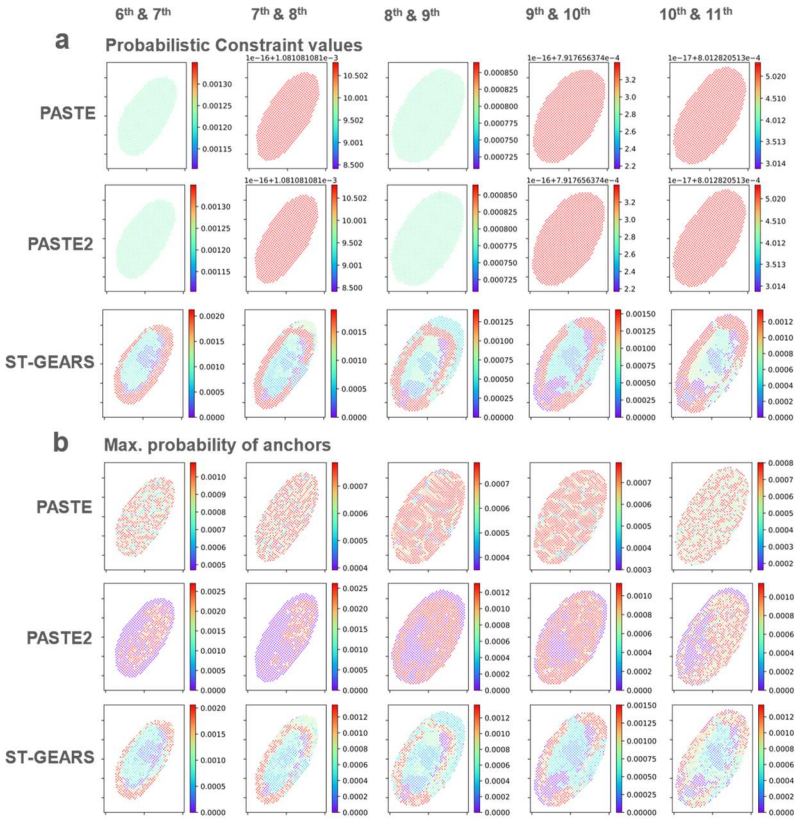

Supplementary Fig. 16: **Distributive emphasis of different cell types of Drosophila embryo induces distributive anchors by ST-GEARS.** (a) In contrast to PASTE and PASTE2, ST-GEARS assigns distributive probabilistic constraints on different cell types of Drosophila embryo as shown on the 1st , 2nd and 3rd row (b) By result, its generated maximum probabilities of spots' anchors are different across cell types, compared to PASTE and PASTE2, as shown on the 4th, 5th and 6th row. Source data are provided as a Source Data file.

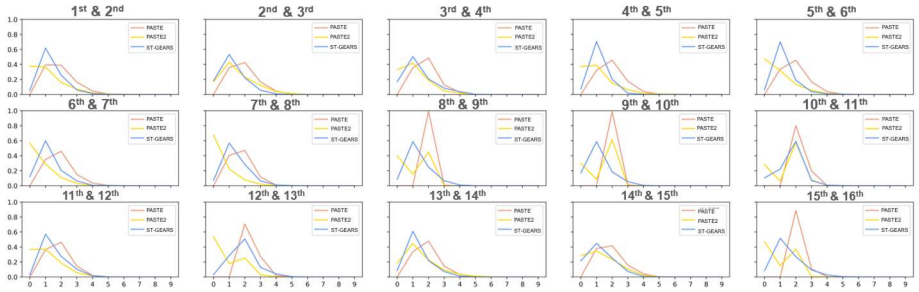

Supplementary Fig. 17: **Suppression of anchors generation on certain spots of Drosophila embryo by ST-GEARS.** Shown here is the comparison of number of anchors distribution of Drosophila embryo dataset computed by PASTE, PASTE2 and ST-GEARS. Each y value shows fraction of no. of anchors specified on x. Different from PASTE, certain percentage of spots have zero anchors generated by ST-GEARS. Source data are provided as a Source Data file.

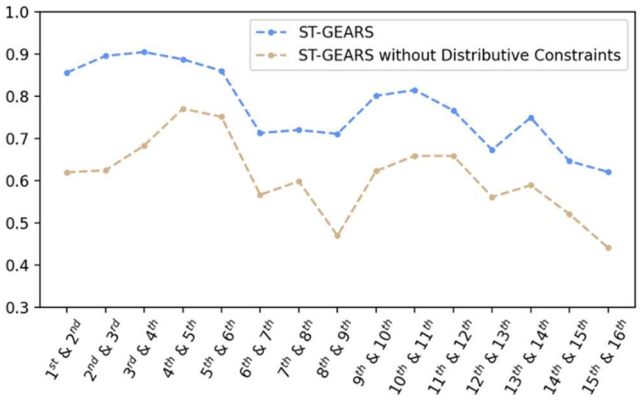

Supplementary Fig. 18: **Mapping accuracy of ST-GEARS with and without Distributive Constraints on registration of Drosophila embryo.** The accuracy index is higher upon DC adopted. Source data are provided as a Source Data file.

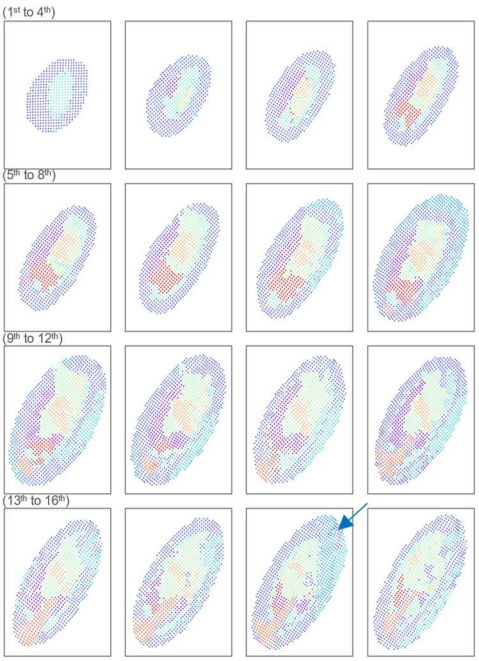

Supplementary Fig. 19: **Individual sections of Drosophila embryo generated by ST-GEARS with Distributive Constraints excluded.** The blue arrow points to section area where experimental flaw remains unfixed by the method. Source data are provided as a Source Data file.

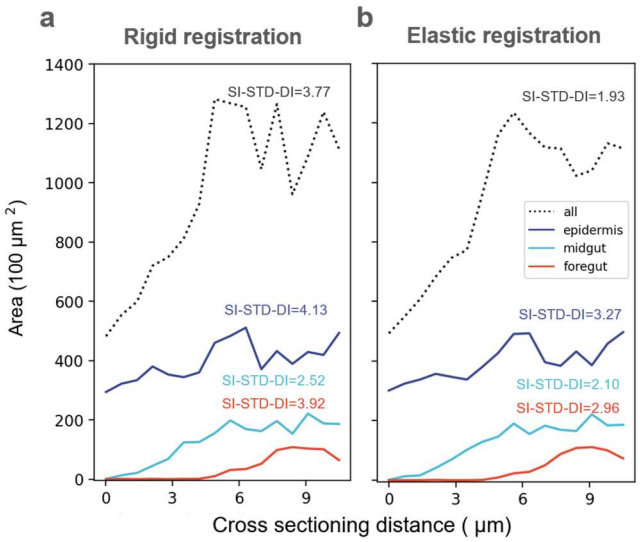

Supplementary Fig. 20: **Elastic registration in ST-GEARS smooths tissue shapes of Drosophila embryo.** (a) Shown here is area changes of epidermis, foregut, and midgut and overall body, along sectioning direction after rigid registration of ST-GEARS. Each area data is calculated based on pixelating the region of tissues, on each registered section, and summing up area of respective pixels. Scale-independent Standard Deviation of Differences (SSI-STD-DI) of each curve is calculated and marked as smoothness index of the curve. (b) Shown here is area changes of the 3 same tissues as (a) and overall body, along sectioning direction after elastic registration of ST-GEARS. Area changes are visually and quantitatively smoother after elastic registration than after rigid registration only. Source data are provided as a Source Data file.

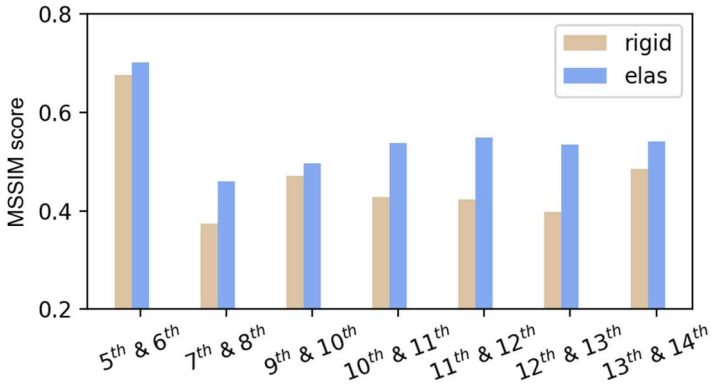

Supplementary Fig. 21: **Elastic registration in ST-GEARS enhances cross-sectional consistency in structurally consistent positions of Drosophila embryo.** Shown here **is** the comparison of Mean Structural Similarity (MSSIM) index of rigid and elastic registration result, of structurally consistent section pairs of Drosophila embryo. The similarity index is higher on elastic than on rigid result. Source data are provided as a Source Data file.

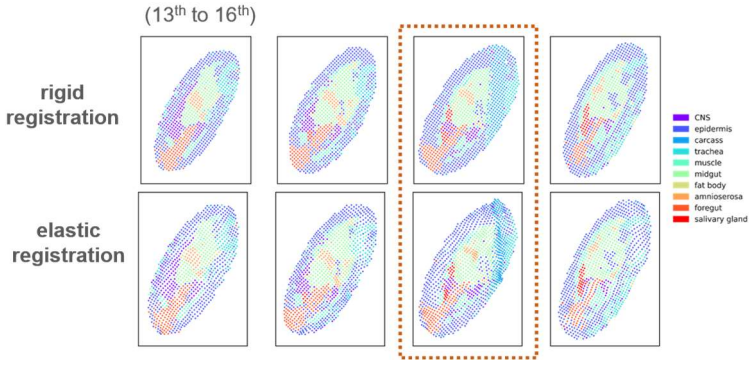

Supplementary Fig. 22: **Elastic registration fixes flaw of Drosophila embryo data.** Top row shows 13th to 16th sections after rigid registration, and bottom row shows corresponding sections after elastic registration. On the 15th section, the flaw region between 2 parallel lines caused during experimental phase was fixed by elastic registration. Source data are provided as a Source Data file.


a
Pre-registered
(1st to 14th)
(15th to 28th)
(29th to 40th)
b
PASTE
(1st to 14th)
(15th to 28th)
(29th to 40th)
c
PASTE2
(1st to 14th)
(15th to 28th)
(29th to 40th)
d
GPSA
(1st to 14th)
(15th to 28th)
(29th to 40th)
e
STalign
(1st to 14th)
(15th to 28th)
(29th to 40th)
f
ST-GEARS
(1st to 14th)
(15th to 28th)
(29th to 40th)
AONm
BLA/PA/TTd
COAp
Car3
ENTl L1
ENTl L2/3
EPd
GABA_1
GABA_2
GABA_3
GABA_4
GABA_5
HIP CA
HIP SUB
HPF SUBd
L2/3 IT
L4/5 IT
L5 ET
L5 IT
L6 CT
L6 IT
L6b
LA
Lamp5
Low Quality
Meis2-like
NP
OB UL
PIR
PPP
Pvalb
RSP
RSP DL
Sst
Sst Chodl-like
TH AD
TH MH
Unclear
Vip/Sncg
empty

Supplementary Fig. 23: **ST-GEARS correctly registers all sections of Mouse brain hemisphere, in contrast to PASTE, PASTE2, STalign and GPSA.** Shown here are all individual 40 sections of, (a) before and after registration by (b) PASTE, (c) PASTE2 (d) GPSA, (e) STalign and (f) ST-GEARS. Positional misalignments are marked by arrows of green, and angular misalignments are marked by arrows of orange. Visible cutting lines used to check angular alignment of result of our method, and mistaken shape distortions by GPSA are marked by dotted lines. While positional misalignments are found in result of PASTE2, and angular misalignments are found in results of PASTE2, PASTE and STalign, neither of the conditions are visible in result of ST-GEARS. Source data are provided as a Source Data file.

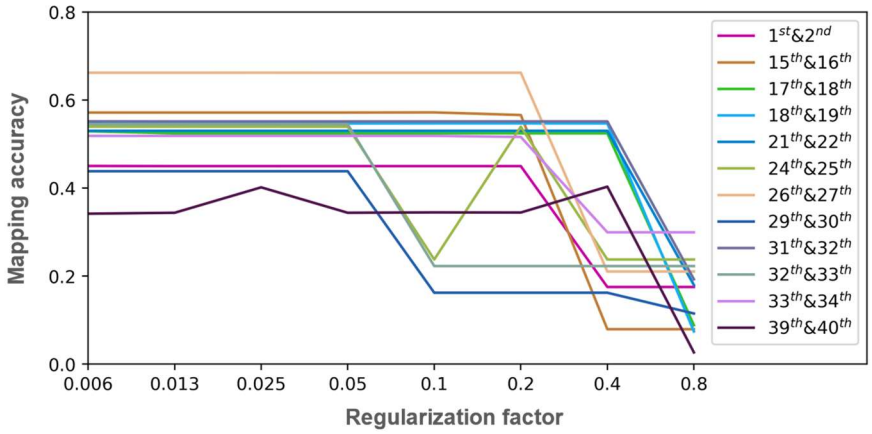

Supplementary Fig. 24: **Self-adaptive regularization generates regularization factor in Mouse brain registration that causes most advanced anchor accuracy.** The figure shows changing mapping accuracy of anchors upon exponentially changing regularization factor. Section pairs with mapping accuracy changes over range of 0.1 are selected and plotted. ST-GEARS runs through the regularization factors, and adopts the factor that causes highest mapping accuracy to ensure a most advanced anchor accuracy. Source data are provided as a Source Data file.

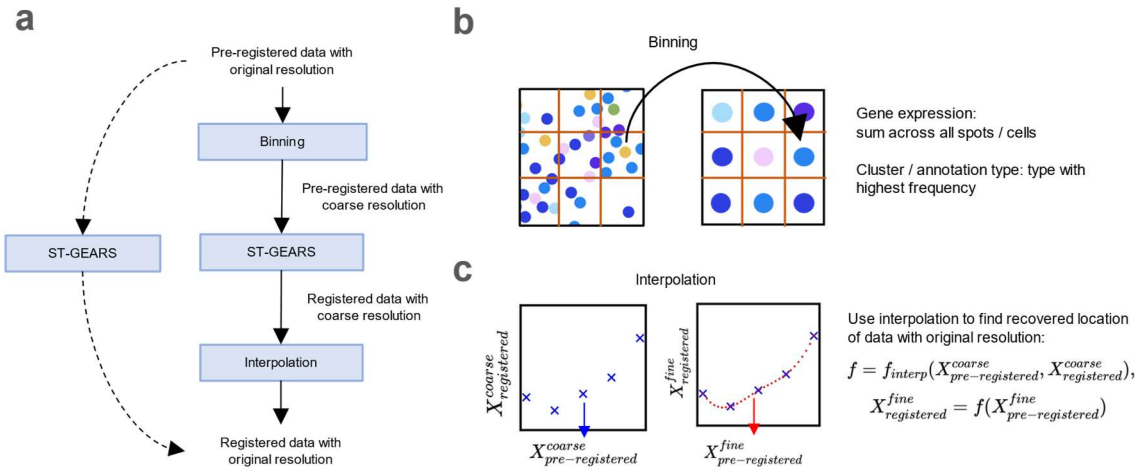

Supplementary Fig. 25: **Granularity adjusting option recommended for datasets with over 3000 spots.** (a) The automatic process of granularity adjusting includes binning the section area, which leads to bin sets that are much less compared to original spots, running the bin sets data with ST-GEARS, leading to registered data with the coarse resolution, and eventually interpolating original resolution data into the coarse one, outputting the registered data with original resolution. (b) In binning step, section area is gridded, with spots squared by each pixel summarized into one single spot. (c) In interpolating step, registered data with original resolution is solved by interpolating the pre-registered original resolution data into pre-registered (output by binning step) and post-registered (output by ST-GEARS step) coarse resolution data.

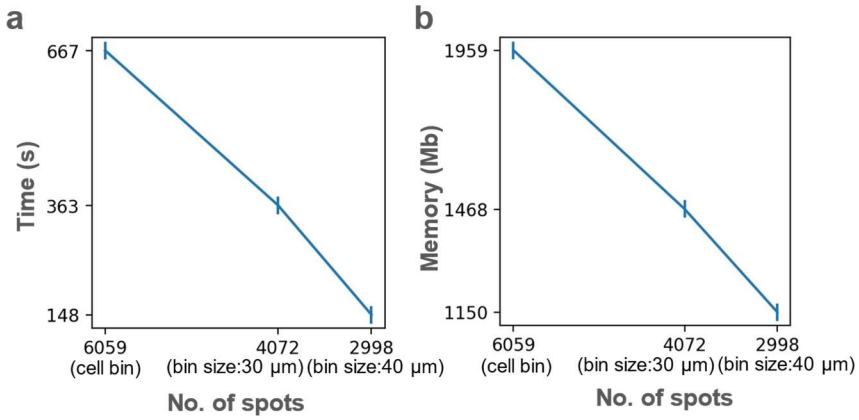

Supplementary Fig. 26: **Time and peak memory consumption by ST-GEARS, and number of spots of different resolutions of Mouse hippocampus.** Shown in (a) is the time consumption comparison and shown in (b) is the peak memory consumption. The different resolution data includes dataset in original resolution of cell bin, the binned data with bin size of 30 μm and the binned data with bin size of 40 μm. Source data are provided as a Source Data file.

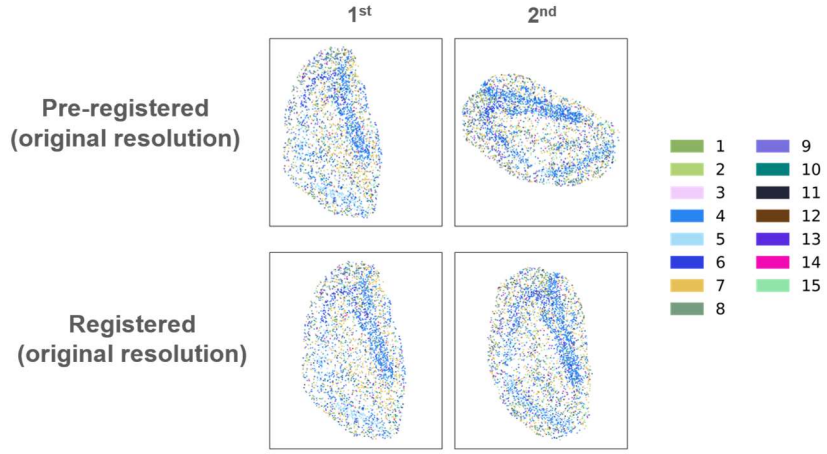

Supplementary Fig. 27: **Pre-registered and post-registered Mouse hippocampus dataset with original resolution.** The 1st row shows pre-registered dataset, and the 2nd row shows registration result of ST-GEARS directly using original resolution, without granularity adjusting adopted. The 1st column represents the 1st section, while the 2nd column represents the 2nd. Source data are provided as a Source Data file.

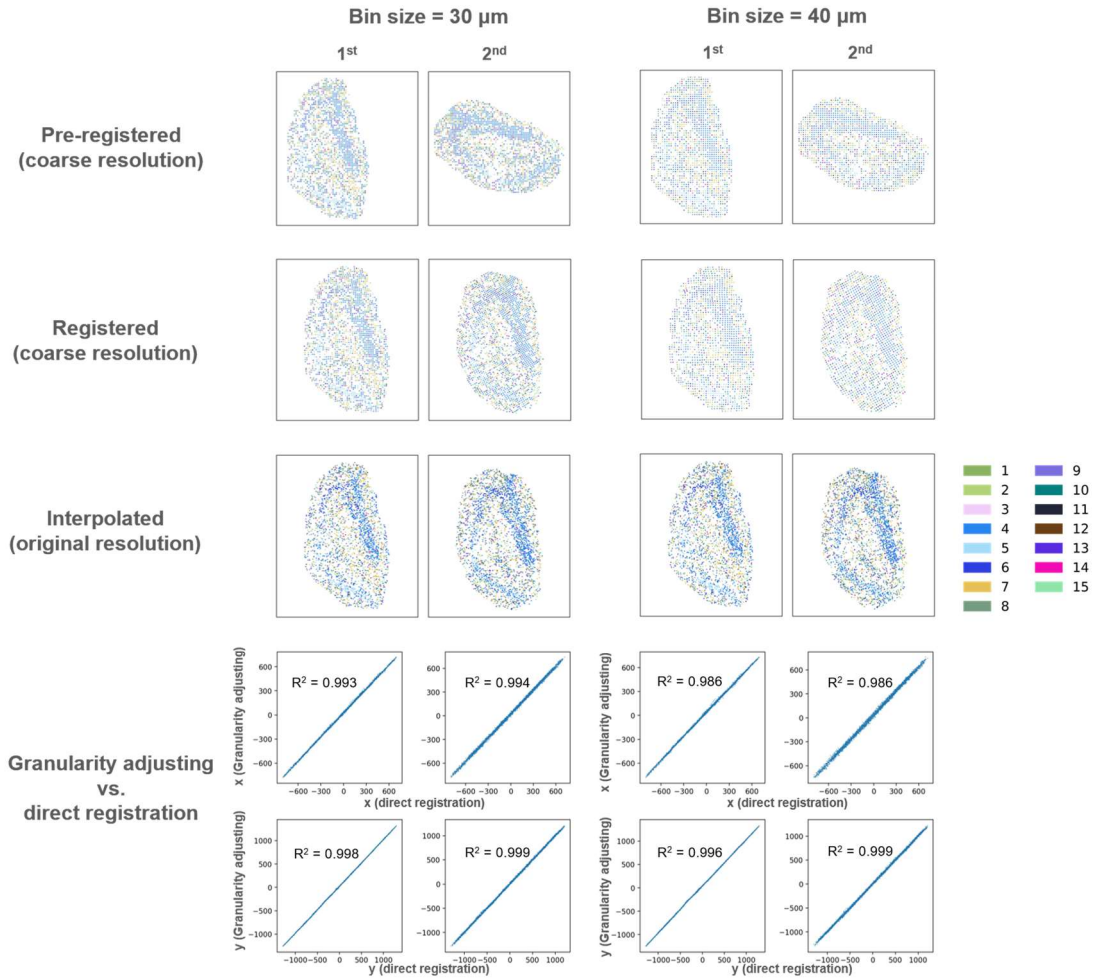

Supplementary Fig. 28: **Registration of Mouse hippocampus dataset with granularity adjusting strategy, in different bin sizes.** From top to bottom presented are binned yet pre-registered datasets, registered binned datasets, interpolation result of dataset with original resolution, and comparison between position of cells by process of granularity adjusting and direct registering through ST-GEARS. Two rows are included in the comparison plots, with the 1st row showing comparison of x coordinates and the 2nd row showing comparison of y coordinates. The 1st and 2nd columns are respectively results of 1st and 2nd sections by bin size of 30 μm in binning step of granularity adjusting, while the 3rd and 4th columns are result of the same two sections by bin size of 40 μm. In comparison between position of cells by process of granularity adjusting and direct registering, the coefficient of determination (R^2) remains over 0.98 across all coordinates, sections, on both bin sizes. Source data are provided as a Source Data file.

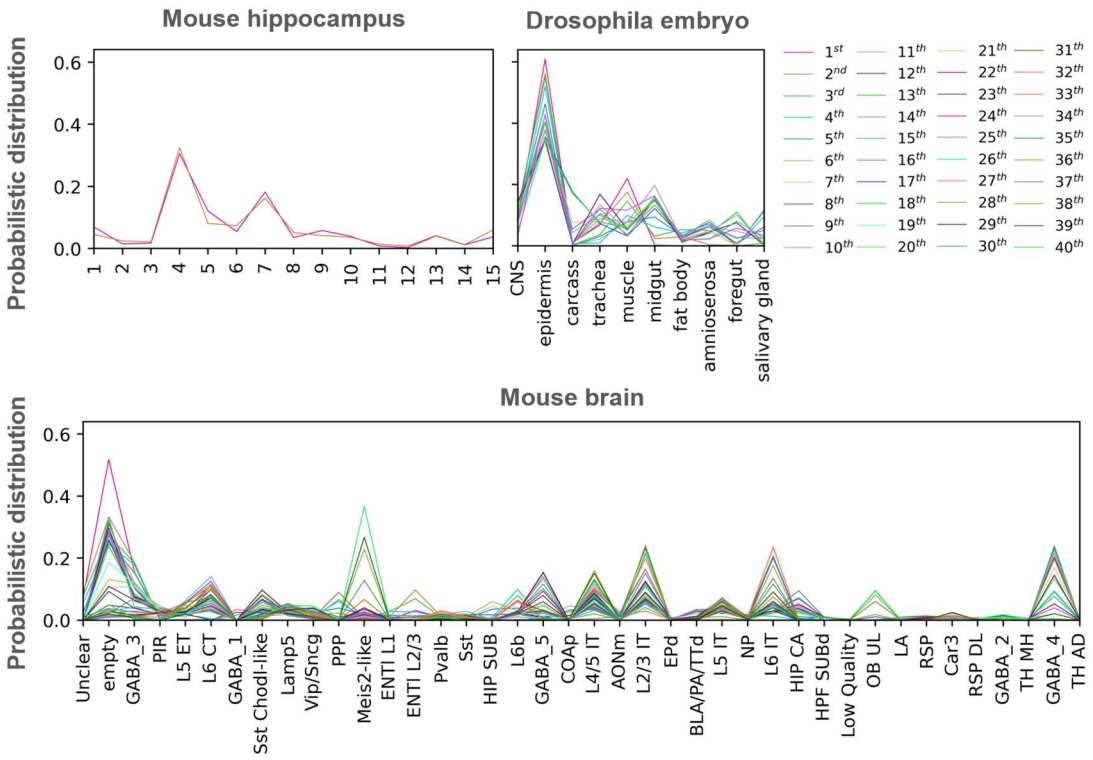

Supplementary Fig. 29: **Probabilistic distribution of proportion of spots on clustering / annotation types, of Mouse hippocampus, Drosophila embryo and Mouse brain datasets.** Each polyline was drawn based on distribution information of a section. Source data are provided as a Source Data file.

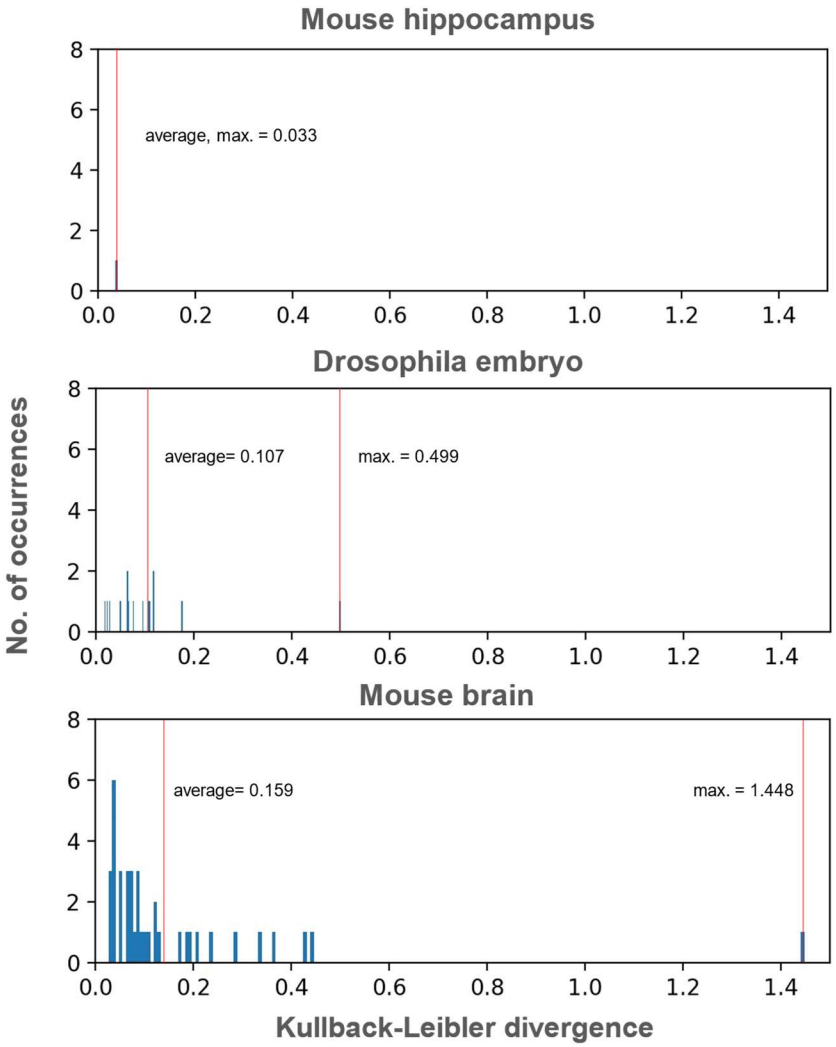

Supplementary Fig. 30: **Histogram of Kullback-Leibler (KL) divergence of probabilistic distribution of no. of spots on different clusters or annotations between closest section pairs, respectively of Mouse hippocampus, Drosophila embryo and Mouse brain datasets.** The position of average and maximum KL divergence was marked by red vertical lines and the respective values were labeled in black. Source data are provided as a Source Data file.

Supplementary Table 1: **ST-GEARS parameters that need to be specified and their value assigned across applications.**

Dataset	Uniform_weight	label_col	pixel_size
Mouse hippocampus	False	'annotation'	10
Drosophila embryo	False	'annotation'	1
Mouse brain	True	'annotation'	200

Supplementary Table 2: Maximum **Kullback-Leibler (KL) divergence of Probabilistic distribution of no. of spots between closest section pairs and whether the Distributive Constraints was adopted in cases of Mouse hippocampus, Drosophila embryo and Mouse brain datasets.**

Application cases	Max. KL divergence	Distributive Constraints adopted
Mouse hippocampus	0.033	True
Drosophila embryo	0.499	True
Mouse brain	1.448	False